

CONSIDERATIONS ON THE HELMHOLTZ RESONATOR SIMULATION AND EXPERIMENT

Iulian LUPEA

Technical University of Cluj-Napoca
E-mail: i_lupea@yahoo.com

The acoustic design by using simulation, in order to bring down the noise level in human surroundings, is of great importance. In the present paper a Helmholtz type resonator is under observation. The first resonant frequency is calculated by using a proper analytical formula. The system composed by the walls and the air filling the cavity and the neck is modeled by using finite elements. Proper boundary conditions are imposed. The acoustic modal analysis is performed and the first couple of acoustic modes are extracted. Each mode is characterized by the natural frequency and the pressure distribution over the system. Finally, the resonator is put into resonance by properly blowing air across its free side of the neck. The resulted sound is observed in frequency domain by using power spectrum analysis. The natural frequencies resulted from the three approaches are compared and are in good agreement. The simulation and the optimization of more complex systems and acoustic materials based on Helmholtz resonators are of great interest and under observation.

Key words: Helmholtz resonator, finite element modeling, acoustic modal analysis.

1. INTRODUCTION

In passive noise control the design of sound absorbers like porous materials, resonators or membrane absorbers are of great interest. Porous absorbers are used primarily for sound in the mid to high frequency and resonant absorbers are used mainly for low frequency absorption. The acoustic design by using simulation, in order to bring down the noise level, plays an important roll.

The Helmholtz resonator is a simple acoustic system consisting of a rigid-walled cavity of volume V , filled with air and a neck of section S and the length L by which the cavity communicates (Fig.1) with the exterior [1, 3, 4, 6]. The air filling the system is under the atmospheric pressure. After a proper short exterior pressure excitation, the air filling the neck is starting to move back and forth damping out in time. The behavior of the air can be approximated and described by a single degree of freedom mechanical vibrating system (Fig.1). The air filling the cavity during the vibration is submitted to condensations and rarefactions acting like a spring and the air located in the tube or neck is acting like an incompressible mass (of air)

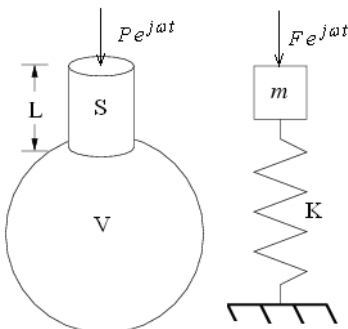


Fig. 1 – Helmholtz resonator.

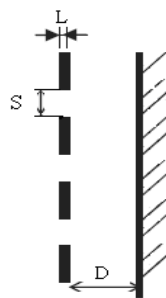


Fig. 2 – MPP.

moving back and forth along the neck. The acoustic wavelength at the fundamental natural frequency is much larger than the cavity and neck's dimensions. This phenomenon has been exploited for thousands of years in making musical instruments. More recently have been used on noise control applications in automotive industry, for mufflers design, the acoustic of habitable, subwoofers, concert halls acoustics or sport halls for enhancement the sound absorption at low frequencies and so on. At the resonance the Helmholtz resonator can be seen as an amplifier.

A plate with multiple holes and equally distanced from a back rigid plate (Fig.2) with an air cavity in-between, forms the Helmholtz absorber or a micro perforated panel (MPP). These absorbers are often mounted on the walls of the rooms where the acoustic pressure is maximum.

The German physicist Hermann von Helmholtz derived the relation by which the first natural frequency of the resonator is calculated. The natural frequency ω_0 associated to the first acoustic mode of the air in the system is:

$$\omega_0 = c\sqrt{\frac{S}{VL}}, \quad (1)$$

where S is the area of the neck's cross-section, V is the volume of the cavity with rigid walls, L is the neck's length and $c = 340\text{m/s}$ is the speed of the sound in air.

The differential equation associated to this system can be derived by observing the displacement of the air mass filling the neck along the neck's axis, applying the Newton's law for the acceleration of this mass, applying gas laws on the air of the cavity the process considered adiabatic, observing the pressures acting on both sides of the 'plug' of air and finally observing the dissipative and the exterior forces when the system is harmonically excited [1, 6]. The resulted differential equation is:

$$\rho SL\ddot{\xi} + R_d\dot{\xi} + (\rho S^2 c^2 / V) \xi = PSe^{j\omega t}, \quad (2)$$

where $\xi(t)$, $\dot{\xi}$ and $\ddot{\xi}$ are the displacement, the velocity and the acceleration of a gas particle along the neck in function of the time t , ρ is the air density, R_d is a dissipative viscous constant, P is the excitation pressure amplitude, ω expresses the harmonic excitation (a complex driving force produced by a pressure wave on the outer end of the neck). While vibrating, through the open end of the neck, the system radiates sound outward resulting a radiation resistance R_r . At the air-neck interface the system presents thermo viscous losses R_i . Both losses of energy are accounted by $R_d = R_r + R_i$. By neglecting the damping and the excitation on relation (2), then dividing by ρSL , the square of the resonator's natural frequency ω_0 as a term multiplying ξ , is obtained.

For the differential equation (2), a more convenient variable $X = S\xi(t)$ (the swept volume) can be considered instead of $\xi(t)$. As well, the relation (2) is divided by S , resulting (3):

$$\frac{\rho L}{S} \ddot{X} + \frac{R_d}{S^2} \dot{X} + \frac{\rho c^2}{V} X = Pe^{j\omega t}. \quad (3)$$

The equation (3) can be written as follows:

$$M\ddot{X} + R\dot{X} + \frac{1}{C} X = Pe^{j\omega t}, \quad (4)$$

where M is the acoustic mass or inertance, R is the acoustic resistance and C is the acoustic capacitance. Relation (4) is similar to the differential equation of the mechanical system composed of the mass, the spring and the damper excited by an harmonic force. Dividing by M the relation (4), removing the excitation and assuming a harmonic solution, the fundamental resonance frequency of the resonator can be extracted:

$$\omega_0 = \frac{1}{\sqrt{MC}}. \quad (5)$$

Neglecting the damping, the Helmholtz resonator is similar to a conservative L - C electrical circuit composed of a capacitor of capacitance C_e connected to the terminals of an inductor of self-inductance L_e . The resonance angular frequency of the electrical oscillations is expressed by an equivalent relation [1]:

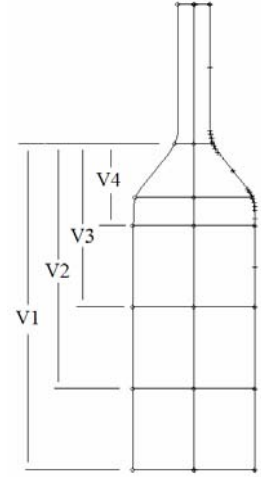


Fig. 3 – Four volumes.

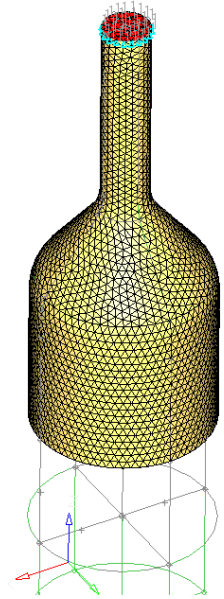


Fig. 4 – Air mesh.

$$\omega_{0e} = 1/\sqrt{L_e C_e}. \quad (6)$$

A correction $L_c = L + a \cdot r$, $1.4 \leq a \leq 1.7$ (extended length of the neck) has to be applied for the neck length L in order to have a better approximation of the natural frequency. This correction constant is properly chosen in function of outer end of the neck. For the flanged end one can use $a = 1.4$ and for the unflanged end $a = 1.7$. The relation (1), becomes:

$$\omega_0 = c \sqrt{\frac{S}{V(L + a \cdot r)}}, \quad (7)$$

where r is the neck radius. This is because an extra small amount of air on both ends of the neck is put into motion during vibration.

The acoustic mass and the acoustic capacitance (8) of the system with a neck of circular section, take the following forms:

$$M = \frac{\rho(L + a \cdot r)}{\pi r^2}, \quad C = \frac{V}{\rho c^2}. \quad (8)$$

The acoustic mass differs from the mass of the air found in the extended neck:

$$M = \frac{\rho(L + ar)}{\pi r^2} = \frac{\rho \cdot L_c}{S} = \frac{\rho \cdot V_{Lc}}{S^2} = \frac{m_{Lc}}{S^2}, \quad (9)$$

where V_{Lc} and m_{Lc} are the volume of the extended neck and the mass of the air in this neck respectively.

By replacing in relation (5) the expression of M and C from (8) and (9), a similar relation for the natural frequency, is derived:

$$\omega_0 = \frac{cS}{\sqrt{V_{Lc} \cdot V}}. \quad (10)$$

When comparing with a single degree of freedom spring-mass system the cavity air plays the spring roll with a spring

constant K :

$$K = \rho S^2 c^2 / V \quad (11)$$

and the mass of the air in the neck is acting like a piston of mass m :

$$m = \rho SL, \quad (12)$$

where $\rho = 1.2 \text{ kg/m}^3$ is the air density. The natural frequency is:

$$\omega_0 = \sqrt{k/m} = c \sqrt{\frac{S}{VL}}. \quad (13)$$

In relation (1) by considering a constant geometry for the neck, results:

$$f_0 = C_{st} \cdot \sqrt{\frac{1}{V}}, \quad (14)$$

where $C_{st} = \frac{c}{2\pi} \sqrt{\frac{S}{L}}$ is considered constant. The relation (14) shows the dependence of the resonant frequency f_0 on the volume change of the cavity. This aspect will be observed by simulation and experiment in the sequel.

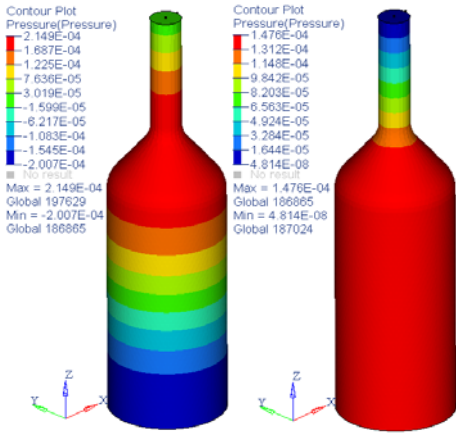


Fig. 5 – 1st and 2nd modes (V1).

2. MODELING THE ACOUSTIC RESONATOR BY USING FINITE ELEMENTS

We are considering a bottle of volume V_{max} of about 750ml. By filling the bottle with water at different levels, one obtains variable air volume for the cavity V . The volume V is bounded by the bottle walls, the water surface and is communicating with the exterior through the bottle's neck ($L = 0.08$ m, $S = 2.6 \cdot 10^{-4}$ m²). First the bottle is filled with water excepting the neck. By using a marked tube of glass a controlled volume of water can be removed from the bottle, resulting the target air volumes V_i , $i = 1, \dots, 4$ (Fig. 3).

In order to model the system under observation the geometry or the CAD model of the air envelope has been created [11]. The cavity walls are meshed by using triangular shell elements. These are structural nodes, each one with six degrees of freedom, three translational and three rotational. The volume (Fig. 4) occupied by the air is meshed by using tetrahedral volume elements, a fixed mesh proper for the fluids [11]. Each node of gas has only one degree of freedom, expressing the pressure at that location. The boundary conditions for the gas are dictated by the structural nodes of the surrounding bottle. For the free nodes at the outer end of the neck, zero pressure has been imposed.

The mesh size is important, limiting the number of the acoustic modes to be modeled. At least six elements per wavelength are recommended. The mesh density of the acoustic model should be able to predict modes up to the upper bound of the frequency of interest. For the fluid model an average element size of 1.5 mm has been proposed. The material model MAT10 has been used to model the properties of the air finite elements. The following parameters are requested in the general case: the bulk modulus, the mass density, the speed of sound, the fluid element damping coefficient and the normalized admittance coefficient for porous material.

Four similar models corresponding to the four different water levels in the bottle have been created.

For each model the volume of the tetrahedral elements is calculated. Then, for each volume the first natural frequency is calculated by using the relation (1) or a similar one filling the appropriate columns in Table 1. From the finite element analysis both the acoustic modes of the air and the structural modes of vibration of the bottle are resulted. The sound absorption can be modeled by using appropriate sound absorbent finite elements [9, 11, 13]. The acoustic absorber element is simulated by an assembly consisting of a mass attached to a spring which is connected in parallel with a damper. The element and its properties are defined by the Chacab and Pacabs card entries, respectively [13]. The Pacabs card entry defines the resistance, reactance and the confidence level of the material. These properties vary in function of frequency and can be measured by using a standing wave tube test (impedance tube). This data is used to calculate the values of the mass, spring, and damper which are introduced in the structural model that will emulate the behaviour of the absorber material. The acoustic absorber element Caabsf and the associated property card Paabsf are used to define a frequency dependent impedance in the fluid-structure interface.

3. ACOUSTIC MODAL ANALYSIS

The acoustic modal analysis simulation is performed by using HyperWorks [11]. For each model at least the first three acoustic modes are observed and the associated natural frequencies are placed in Table 1.

The pressure distribution of the air in the system (the cavity and the neck) is obtained for each acoustic mode. The pressure distribution for the first acoustic mode and the second acoustic mode at the maximal volume ($V_1 = 691 \cdot 10^{-6}$ m³) are presented in Fig. 5. For the first mode, at the base of the bottle, the variation of the pressure (amplitude) is high and the air particle displacement is small. At the opposite (free) end the pressure variation is small and the displacement of the air particles is large, the air traveling back and forth through the neck with the frequency associated to the first acoustic mode. When the air is traveling toward exterior the pressure in the bottle is less than the atmospheric pressure and *vice-versa*. In a similar manner one can observe the pressure and the displacement of the air particles for other modes. The third acoustic mode (volume V_1) pressure distribution and two zero pressure surfaces (nodes) are visualized in Fig. 6. For the second acoustic mode only one zero-crossing pressure surface is observed.

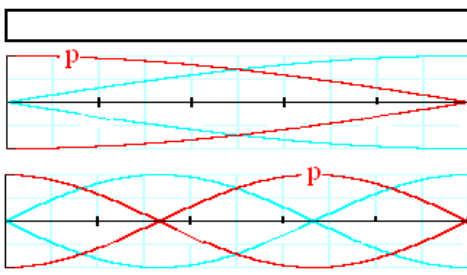


Fig. 7.

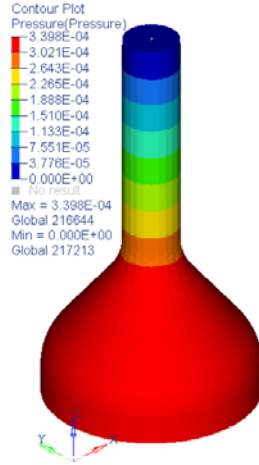


Fig. 8 – V4, mode #1.

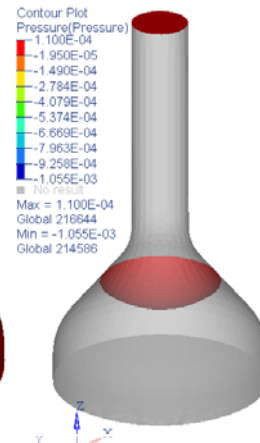


Fig. 9 – V4, acoustic mode #2.

Table 1

Results for the resonator $r=0.000924$ [m]; $S=0.000268$ [m²]

First 2-3 natural frequencies [Hz]	Volume V [m ³]*e-6	First natural frequency [Hz]		
		Calculated rel. (1)	Calculated rel. (6) a=1.5	Measured
f1=112.5 , f2=990.2, f3=1796.1	V1=659	f1=121	f1=112	f1=119
f1=132.8 , f2=1336, f3=1926	V2=478	f1=142	f1=131	f1=140
f1=169 , f2=1799.5	V3=297	f1=180	f1=167	f1=177
f1=268 , f2=1942	V4=115.8	f1=289	f1=267	f1=273

The pressure sign variation for each of the first three modes is as follows:

Mode #1: | OE=0, - - | or | OE=0, + + |, where OE stands for Open End where the pressure variation is zero, the pressure equals the atmospheric pressure. A minimum pressure of $-1.476 \cdot 10^{-4}$ can be observed in Fig. 5 (this is not a real pressure, being part of the scaled pressure distribution of the acoustic mode).

Mode #2: | OE=0 - - 0 + + | or | OE=0 + + 0 - - |

Mode #3: | OE=0 + + 0 - - 0 + + | or | OE=0 - - 0 + + 0 - - |.

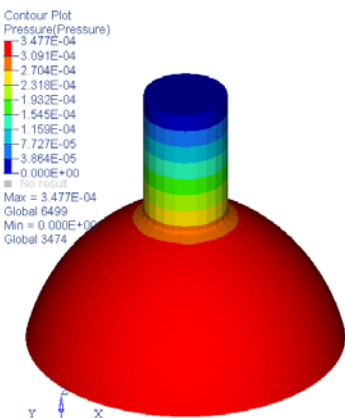


Fig. 10 – Short neck, mode #1.

At a maximum of the pressure the particle velocity is minimal and *vice-versa*. Absorbers are recommended to be placed in locations where the velocity is important. At the fluid level (hard bound) the pressure is maximal and the particles speed is zero. The pressure variation is similar to the pressure in a tube with an open end and the other one closed (Fig. 7).

For the smallest volume $V_4 = 115.8 \cdot 10^{-6}$ m³, the first acoustic mode is depicted in Fig. 8 and the second acoustic mode in Fig. 9.

A second bottle with a short neck ($L = 0.035$ m, $S = 3.66 \cdot 10^{-4}$ m²) it was observed for the same four volumes of air. The same steps are followed and the results have been centralized. The results are slightly less precise comparing to the first case. The first acoustic mode for the smallest volume $V_4 = 116e-6$ m³ is depicted in Fig. 10. The frequency associated to this mode is about 440 Hz. Placing a tuning fork in vibration at the outer end of the neck the system resonates, amplifying the tone.

4. EXPERIMENTAL PROCEDURE

The frequencies calculated above (with relations and by simulation) will be compared with experimental values. The first acoustic mode can be excited by touching with the lower lip and blowing across the bottle neck by using a proper angle. The blowing intensity should be soft in order to excite the first acoustic mode. The frequency associated with the first acoustic mode can be heard.

An acquisition system based on the Labview software and a PC dynamic signal analysis board type NI PCI 4451 has been used for measuring the resulted sound [12]. The application acquires the sound continuously, by blocks, from one channel to which a PCB microphone, ICP type, is connected. The scan rate has to be selected properly. The time signal [V] is scaled to pressure [Pa] and converted to frequency domain by using FFT analysis followed by the power spectrum calculation. The system has been calibrated with a Larson Davis calibrator (94 dB and 114 dB at 1000 Hz).

A transient type analysis has been used. The associated Power spectrum (dB rms, reference pressure $P_0=20 \cdot 10^{-6}$ Pa) analysis diagram has been observed.

A Labview acquisition and processing application has been used and run on a PC computer [8]. After the typical Labview functions AI Config.vi and AI Start.vi for acquisition setting up, a While loop to read repeatedly scan blocks from the intermediate buffer, is used. The application diagram is depicted in Fig. 11. The acquired signal is visualized in time domain and the calculated power spectrum is sent continuously to the screen. On the front panel of the application an intensity chart can be monitored as well, in order to have an overview of the power spectrum variation in time.

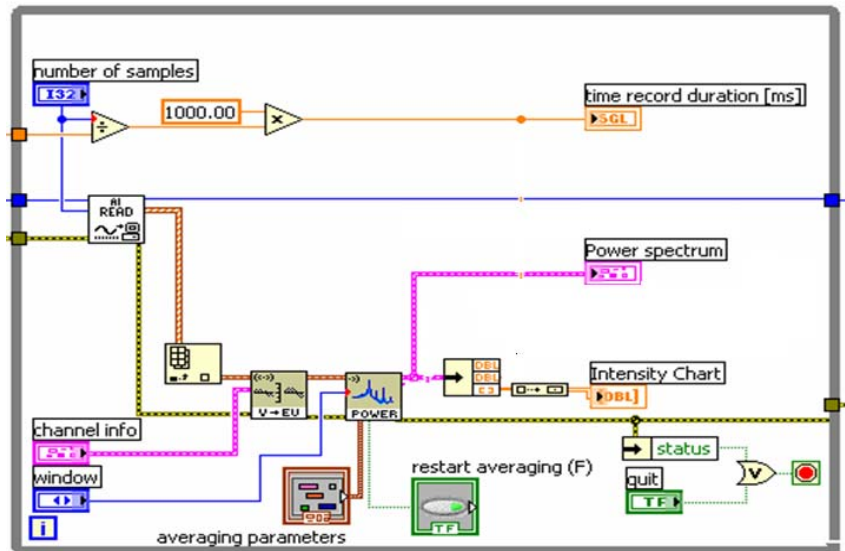


Fig. 11 – Labview application's diagram (partial).

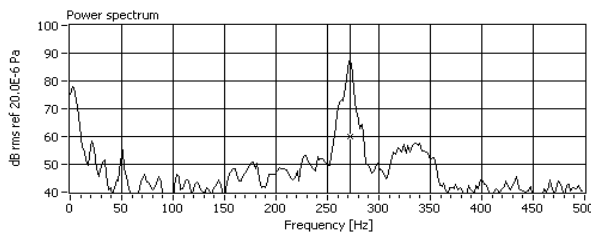


Fig. 12 – Long neck: $V = 116\text{ml}$, mode#1 273Hz.

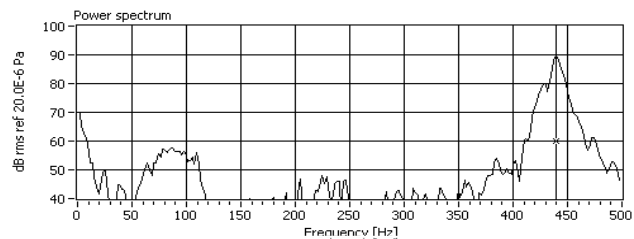


Fig. 13 – Short neck: $V = 116\text{ml}$, mode#1 440Hz.

The Peak Hold average type permitted to freeze the highest peaks on the screen and to read, by using a cursor, the associated resonant frequency. Linear and exponential averaging types are also available. Typical power spectrum graphs are depicted in Figs. 12 and 13, for the bottle with a long neck and for the one with a short neck.

5. CONCLUSIONS

A Helmholtz resonator has been observed from analytical, simulation and experimental points of view. A micro perforated panel usually composed of a plate with multiple holes and equally distanced from a back rigid plate with an air cavity in-between can be seen as a collection of interconnected Helmholtz resonators.

The volume of one resonator has been modified taking four different values. For each particular system the value of the fundamental resonant frequency calculated by using a classical formula and the values resulted from simulation and experiment are in good agreement. Resonators with the same characteristic features are similar in case the shape of the cavity V changes. The acoustic modal analysis by using finite elements is proposed to be a good and confident approach in observing acoustic systems with applications in developing and optimizing acoustic material and structures. Phenomena like acoustic absorption and transmission loss encountered in the real structures can be included in the simulation by using acoustic absorber and acoustic barrier finite elements. The resistance, reactance, frequency-dependent impedance and the confidence level of the acoustic materials can be considered, as well in a future work. The simulation and optimization of more complex systems and acoustic materials based on Helmholtz resonators are under observation and of great interest.

REFERENCES

1. Bădărău, E., Grumăzescu, M., *Bazele acusticii moderne*, Edit. Academiei RPR, 1961.
2. Duhring, M., Jensen, J., Sigmund, O., *Acoustic design by topology optimization*, Journal of sound and vibration, **317**, 2008.
3. Everest F., Pohlmann, K., *Master handbook of acoustics*, McGraw Hill, 2009.
4. Fahy, F., *Foundation of engineering acoustics*, Elsevier Academic Press, 2005.
5. Kim, H., Cha, J., Song, G., *Geometric and number effect on damping capacity of Helmholtz resonators in a model chamber*, Journal of sound and vibration, **329**, 2010.
6. Lawrence, E., Austin, R., Coppens, A., *Fundamentals of acoustics*, John Wiley & Sons, Inc. New York, 2000.
7. Lee, Y., Sun, H., Guo, X., *Effects of the pane and Helmholtz resonators on a micro-perforated absorber*, Int. J. of Appl. Math. and Mech., **4**, 2005.
8. Lupea, I., *Vibration and noise measurement by using Labview programming*, Casa Cărții de Știință, Cluj-Napoca, 2005.
9. Lupea, I., Szathmari, R., *Vibroacoustic frequency response on a passenger compartment*, J. of Vibroengineering, Kaunas, Lithuania, **12**, 4, Dec. 2010.
10. Maluski, S., Gibbs, B., *Application of a finite-element model to low-frequency sound insulation in dwellings*, J. Acoust. Soc. Am., **108**, 4, Oct. 2000.
11. ** HyperWorks Altair Engineering, Troy, MI, USA.
12. ** Labview 8.6, National Instruments, Austin, Texas, USA.
13. ** MSC Nastran, User's Manual and Quick Reference Guide; MSC Software Corporation, USA.

Received September 16, 2011